

A Method for PIO Suppression in Aircraft with Fly-By-Wire Controls: System Development and Validation via Flight Simulator Tests

Rafael Morales Miranda¹ , Jorge Henrique Bidinotto^{1,*} 

¹Universidade de São Paulo  – Escola de Engenharia de São Carlos – Departamento de Engenharia Aeronáutica – São Carlos/SP – Brazil.

*Correspondence author: jhbidi@sc.usp.br

ABSTRACT

This article introduces a technique for suppressing pilot-induced oscillations (PIO) in aircraft equipped with fly-by-wire (FBW) flight controls. Drawing from the real-time oscillation verifier (ROVER) concept proposed by Mitchell and Hoh, in 1994, and an adaptive suppression system by Moura in 2018, the method involves dynamically adjusting stability derivatives via software during aircraft operation. The ROVER detects PIO conditions during flight, directing changes to the aircraft's dynamics. Switching to a less susceptible model during PIO mitigates oscillations. The study focuses exclusively on longitudinal motion and pitch angle control. The proposed system is implemented and simulated using MATLAB routines, complemented by human pilot trials on a flight simulator. Results demonstrate real-time detection of PIO oscillations and effective mitigation, ensuring system integrity with acceptable degradation in flight qualities during transitions.

Keywords: Pilot-induced oscillation; Fly-by-wire; Adaptive control; Real-time operation.

INTRODUCTION

With the increasing use of digital computers in aircraft flight control systems, the architecture named digital fly-by-wire (FBW) allowed the implementation of different dynamics in those systems via software. These dynamics can be modeled using different methods, such as the stability and control derivatives. However, this kind of system inherited many of the drawbacks of manual flight control aircraft, such as the phenomenon designated as pilot-induced oscillations (PIO). This phenomenon can be defined as sustained oscillations that are a result of inadvertent between the pilot and the aircraft inadvertently (USDoD 1995) and is caused mainly by high gain on yoke (or stick) inputs, delay in flight controls response, or by position limitation of the control surface actuators.

The main problem in events like these is that they cannot always be avoided and that there is no “pre-PIO situation,” so it cannot be detected before the oscillations start. Despite the significant number of works carried out since the 1960s, such as Anderson (1998), Ashkenas *et al.* (1964), and Smith and Berry (1975), this phenomenon still occurs, and its occurrence typically leads to severe in-flight commercial and military aircraft accidents (Bidinotto and Almeida 2021). The challenge of finding an effective algorithm to perform real-time detection of this phenomenon, and primarily its suppression (or mitigation), remains open.

Received: Jan. 18, 2024 | **Accepted:** Dec. 24, 2024

Peer Review History: Single Blind Peer Review.

Section editor: Valder Sttefen 



Furthermore, few research works use adaptive control theory for linearized control, such as Sun *et al.* (2016), but no research was found to suppress this kind of phenomenon in FBW systems.

Some applications for nonlinear PIO control are proposed by Harmin and Cooper (2011), Paladini *et al.* (2024), and Tran *et al.* (2017). A PIO flight experience is described by Lee (2000), which shows that this topic is still relevant and a concern for both industry and academia. These proposals are generally theoretical and present the ideal solution to the problem, but a practical implementation and application remain current problem.

Moura (2018) and Moura *et al.* (2018) developed and implemented an adaptive control system able to detect and suppress the PIO oscillations with good theoretical results, using pilot mathematical models whose behavior during PIO occurrence is explored and detailed by Bidinotto *et al.* (2022).

Considering this scenario, the present work proposes an extension of this adaptive control (Moura 2018), switching critical values of the state matrix (A_1) to a low proneness one (A_2) in real-time during a task of PIO detection and suppression. The considered motion axis for this work is the longitudinal dynamics, focusing on models for pitch motion.

The objective of this work is to propose a system capable of detecting and avoiding a PIO condition in real-time, in addition to being implemented in aircraft with FBW commands. The system was tested in flight simulators and validated with 10 volunteers, comparing their performance in task accomplishment with and without using this system.

This paper is structured as follows: the aircraft modeling process is discussed first, followed by a detailed description of the proposed control system, including the ROVER algorithm. Next, the methodology applied in the simulations is outlined. The subsequent section presents the results and provides a discussion, with the paper concluding in the final section.

Aircraft modelling

The standard six degrees of freedom rigid body linear model defined by Etkin and Reid (1996) is used, considering a constant throttle condition. In this model, the aircraft is considered to perform translational movements along each axis and rotational motion angles (roll (ϕ), pitch (θ), and yaw (Ψ)). The resultant aerodynamic forces can be denoted by its components $[X, Y, Z]$ and the resultant moment vector $[L, M, N]$. The aircraft's CG has translational velocity $[u, v, w]$ and angular velocity $[p, q, r]$. The resulting linear equations of longitudinal motion are then expressed using the state space methodology, as in Eq. 1, where the vector represents the states $x = [(\Delta u \ w \ q \ \Delta \theta)]^T$. For longitudinal motion, matrices A and B have the elements given by Eqs. 2 and 3, respectively, where the terms $X_u, X_w, Z_u, Z_w, Z_q, Z_{\dot{w}}, M_u, M_q$ and $M_{\dot{w}}$ denote the longitudinal dimensional stability derivatives whereas $X_{\delta_e}, Z_{\delta_e}$ and M_{δ_e} define the longitudinal control derivatives, while g is the gravity acceleration, m the aircraft mass, and I_y the moment of inertia related to pitch movement. These derivatives can also be expressed in a non-dimensional form, which will be used in the present work by the terms $C_{x_u}, C_{x_{\dot{\alpha}}}, C_{z_u}, C_{z_{\alpha}}, C_{z_q}, C_{z_{\dot{\alpha}}}, C_{m_u}, C_{m_{\alpha}}, C_{m_q}, C_{m_{\dot{\alpha}}}$ when referring to the stability derivatives and $C_{x_{\delta_e}}, C_{z_{\delta_e}}$ and $C_{m_{\delta_e}}$ for the control ones. These values will be divided later between "original dynamics" and "low proneness."

The matrix C is defined as identity, resulting in the output vector y being identical to the state vector x , and D is considered a null column matrix. The vector u is the input vector, which in this case represents only the elevator input:

$$\begin{cases} \dot{x} = Ax + Bu \\ y = Cx + Du \end{cases} \quad (1)$$

$$A = \begin{bmatrix} \frac{X_u}{m} & \frac{X_w}{m} & 0 & -g \cos \theta_o \\ \frac{Z_u}{m-Z_{\dot{w}}} & \frac{Z_w}{m-Z_{\dot{w}}} & \frac{Z_q + mu_o}{m-Z_{\dot{w}}} & \frac{-mg \sin \theta_o}{m-Z_{\dot{w}}} \\ \frac{1}{I_y} \left[M_u + \frac{M_{\dot{w}} Z_u}{(m-Z_{\dot{w}})} \right] & \frac{1}{I_y} \left[M_w + \frac{M_{\dot{w}} Z_w}{(m-Z_{\dot{w}})} \right] & \frac{1}{I_y} \left[M_q + \frac{M_{\dot{w}} (Z_q + mu_o)}{(m-Z_{\dot{w}})} \right] & -\frac{M_{\dot{w}} mg \sin \theta_o}{I_y (m-Z_{\dot{w}})} \\ 0 & 0 & 1 & 0 \end{bmatrix} \quad (2)$$

$$B = \begin{bmatrix} \frac{X_{\delta_e}}{m} \\ \frac{Z_{\delta_e}}{m-Z_{\dot{w}}} \\ \frac{M_{\delta_e}}{I_y} + \frac{M_{\dot{w}}}{I_y} \frac{Z_{\delta_e}}{(m-Z_{\dot{w}})} \\ 0 \end{bmatrix} \tag{3}$$

$$u = [\delta_e] \tag{4}$$

The longitudinal aircraft models implemented in this work are derived from reference flight data of the Boeing 747-100 model in a cruising horizontal flight condition at an altitude of 40,000 ft and a Mach number of 0.8, as stated by Etkin and Reid (1996). The stability and control derivatives for this flight data are shown in Table 1, and the resultant aircraft model with this data is denoted as model A_1 .

Table 1. Boeing 747-100 model stability and control derivatives.

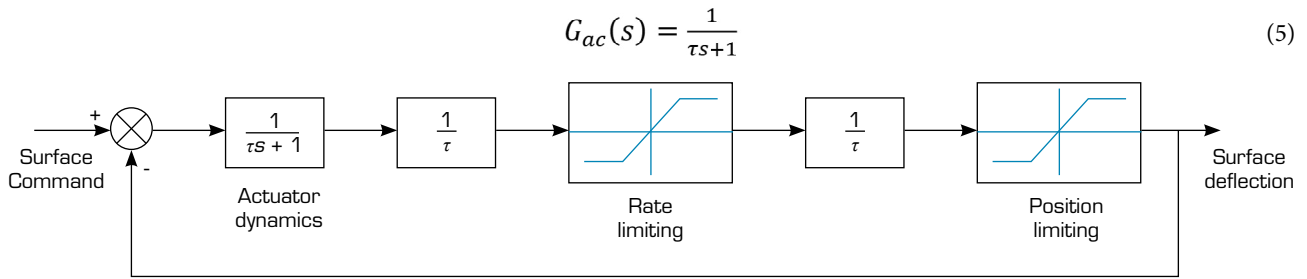
Derivatives	Original (A_1) Etkin and Reid (1996)	Low (A_2) Moura et al. (2018)
C_{x_u}	-1.08×10^{-1}	-
C_{x_α}	2.193×10^{-1}	-
C_{z_u}	-1.4139	-
C_{z_α}	-4.92	-
C_{z_q}	-5.921	-
$C_{z_{\dot{\alpha}}}$	5.896	-
C_{m_u}	1.043×10^{-1}	-
C_{m_α}	-1.023	-
C_{m_q}	-23.92	-70
$C_{m_{\dot{\alpha}}}$	-6.314	-52
$C_{x_{\delta_e}}$	-1.653×10^1	-
$C_{z_{\delta_e}}$	-1.579×10^6	-
$C_{m_{\delta_e}}$	-5.204×10^7	-

Source: Elaborated by the authors.

Moura *et al.* (2018) list a set of seven derivatives that influence diminishing the proneness of the aircraft to the PIO phenomenon, as well as their value ranges to give this behavior. Based on this work, some empirical tests were performed in the flight simulator (described in the Suppression adaptive control system design section), trying to switch the lowest number of different derivatives, testing different sets and values for the proposition of a model with low proneness to PIO, indicated by matrix A_2 . The derivatives for this model are shown in Table 1 with the different values added. The values not shown in the column of model A_2 are the same as those used for A_1 .

A simple actuator servo-hydraulic model was incorporated into the system to simulate an aircraft faithful to reality. It enables modeling the rate and position saturation of the actuator system and can be described as shown in Fig. 1. When the commands are of small amplitude, Eq. 5 describes the actuator's dynamics.



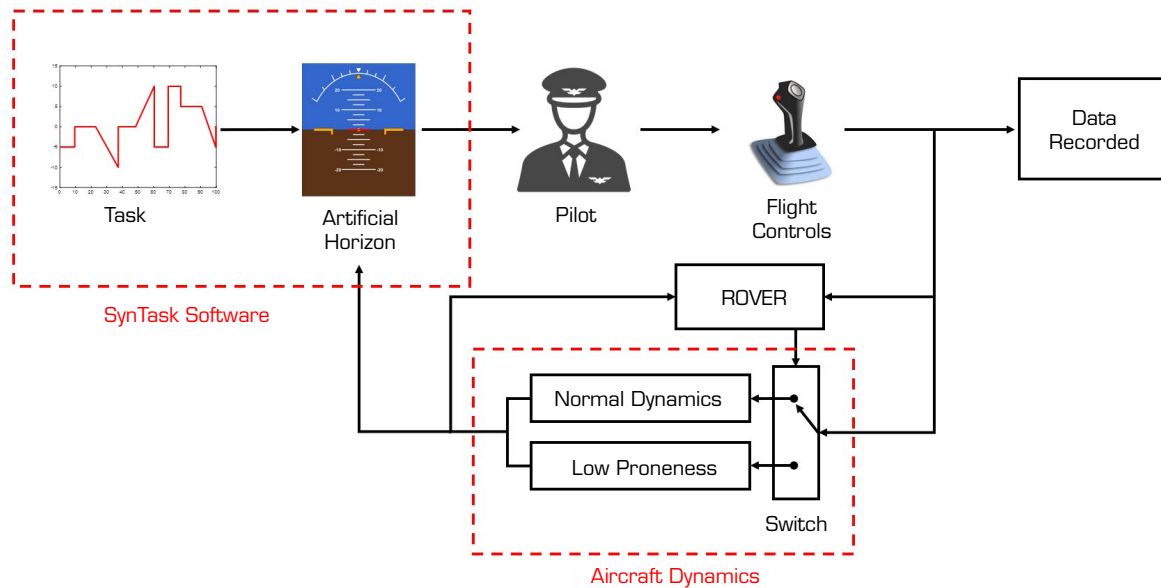


Source: Elaborated by the authors.

Figure 1. Aircraft surface actuator model.

Suppression adaptive control system design

The diagram in Fig. 2 presents the adaptive control system architecture and the various parts and systems involved in the experimental setup. Each element shown in the Fig. 2 is detailed below.



Source: Elaborated by the authors.

Figure 2. Suppression control system architecture.

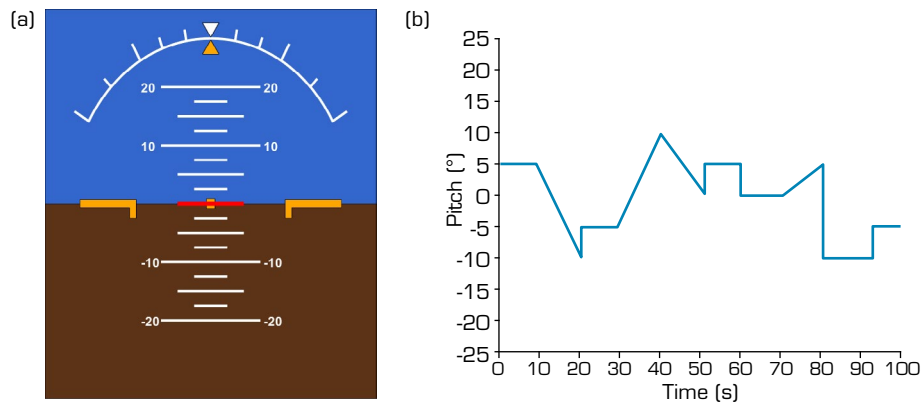
Syntask software

Syntask software was developed at Aeronautics Engineering Department from São Carlos School of Engineering – USP and registered by BR512022002377-6. Developed in MATLAB, the software consists of an interface based on an artificial horizon with a red line representing the task the pilot must follow using a joystick, as shown in Fig. 3a. The software allows changes in the applied task and aircraft dynamics, with minor modifications to the code. Figure 3b shows an example of a task that can be adjusted or modified to requirements of the test.

Pilots and flight controls

For the tests, 10 volunteers participated. None of them had experience with piloting, which was considered advantageous for the study. The objective was to compare pilot performance with and without using the proposed adaptive control system.

Experienced pilots might recognize and/or avoid PIO situations more easily. Since the primary focus of the paper is to test the methodology, the authors consider the use of non-experienced pilots a more conservative approach. Test procedures are described in the Methodology section.



Source: Elaborated by the authors.

Figure 3. Artificial horizon, highlighting the line to be followed (a), and an example of a possible task to be performed (b).

The control used in the simulation was a Thrustmaster Harthog flight stick, commonly used in flight simulation, as shown in Fig. 4.



Source: Elaborated by the authors.

Figure 4. Thrustmaster Harthog flight stick used in tests.

ROVER

The real-time oscillation verifier (ROVER) was first defined by Mitchell and Hoh (1994) and later implemented in works such as Johnson (2002), Liu (2012), and Mitchell *et al.* (2004). This method detects, in real-time, whether the PIO phenomenon is occurring by monitoring four parameters: (i) frequency of pitch rate; (ii) amplitude of aircraft response; (iii) amplitude of pilot commands; and (iv) phase angle difference between pilot input and aircraft response. When all parameters exceed the threshold values listed in Table 2, their corresponding flag is set to 1 (TRUE). Otherwise, the standard value is 0 (FALSE). A PIO condition is detected once TRUE classification is reached in all parameters. Threshold values presented in Table 2 were chosen following the limits defined by Liu (2012) to avoid detections lasting less than 1 second.

Table 2. ROVER parameters.

Parameter	Threshold value
Pitch rate magnitude	$\geq 6^\circ \cdot s$
Pitch rate frequency	0.85-10 rad·s
Pilot command	≥ 1.0 (peak-to-peak)
Phase difference	$\geq 80^\circ$

Source: Elaborated by the authors.

Aircraft dynamics

Once the ROVER algorithm detects a PIO condition, the suppression system is activated via an electronic switch, with a transition time of 1.5 seconds. During this period, the non-dimensional derivatives C_{mq} and $C_{m\dot{\alpha}}$ change their values linearly from model A_1 to A_2 (Table 1), avoiding system instability during simulation, by passing through 30 intermediate values until getting their final value. If the ROVER is set as TRUE and back to FALSE in less than 1.5 seconds, the value of derivatives stops changing and returns to the original value in the same ratio.

This setting (linear, with 1.5 seconds of changing time) was determined empirically, trying to affect as minimum as possible the flying qualities during the values transition. As soon as the aircraft leaves PIO condition (ROVER = FALSE), the system returns gradually to model A_1 , passing through the same intermediate values also in 1.5 seconds.

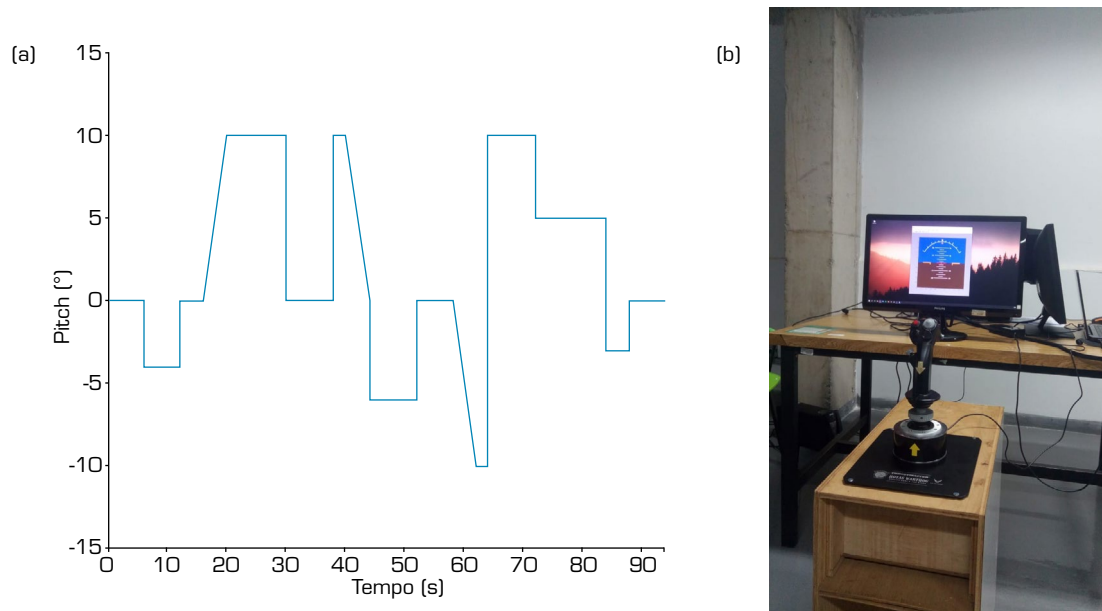
Data recorded

Data were recorded at an acquisition rate of 0.05 seconds for each trial. The recorded parameters included:

- Time, in seconds;
- Task to be followed, in degrees;
- Pilot input (stick deflection), in degrees;
- Aircraft response (pitch angle), in degrees;
- ROVER (Boolean value: 1 for PIO condition, 0 for non-PIO).

METHODOLOGY

To test the influence and functionality of the suppression system, 10 volunteers with no experience in piloting were tested. They received a briefing about the task to be followed using the Syntask platform (Fig. 5a). However, they were not informed about the suppression system or its existence. Each volunteer followed the pitch task shown in Fig. 5b, for 10 repetitions – five with and five without the system, in a randomized order.



Source: Elaborated by the authors.

Figure 5. Task used during tests (a) and test bench (b).

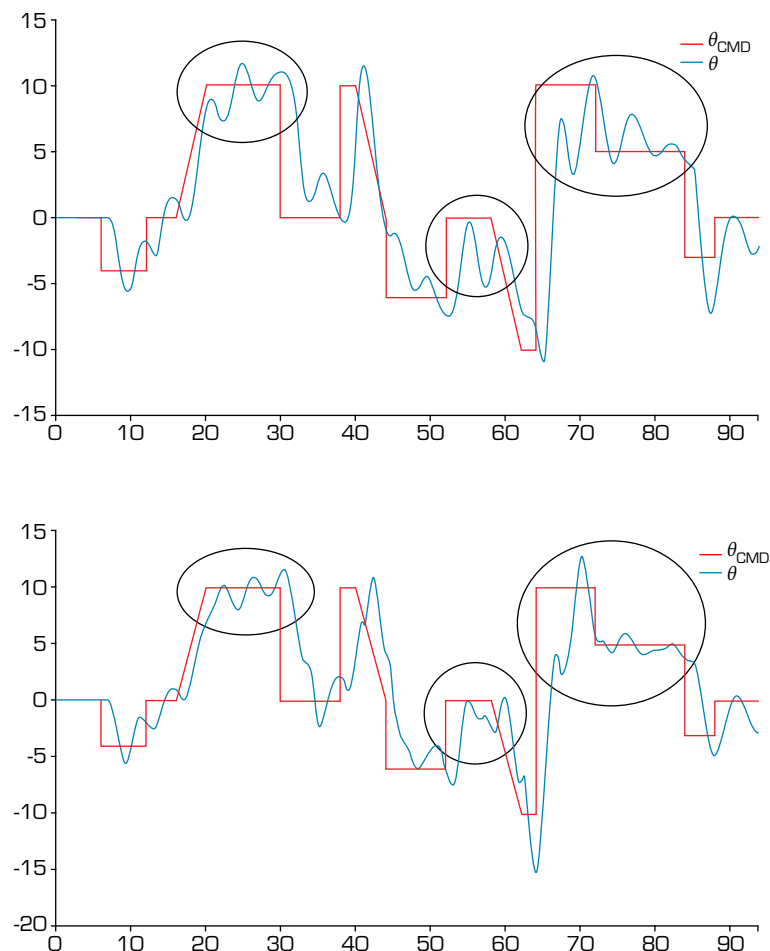
Despite the volunteers' task learning (which was always the same), the focus of the experiments was the comparison between using or not using the system, so the procedure was considered consistent enough to validate its functioning.

Studies like Chase (1967) suggest that the use of motion-based simulators stimulate the functioning of the vestibular system in conjunction with the visual system. The result is that with motion bases, pilots have a reduced tendency to overreact during a maneuver. Thus, for a maneuver like PIO, the use of fixed-base simulators makes the pilot-aircraft system more susceptible to the emergence of the phenomenon, making the validation of the PIO suppression methodologies more conservative and requiring the system to be more robust.

RESULTS AND DISCUSSION

Temporal series from the experiments showed a significant difference between the pilots' behavior when acting with and without the suppression system during a task. Figures 6a and b show the results from one of the volunteers, without and with the system, respectively.

It is essential to note that these trials presented correspond to the same volunteer in consecutive tasks to emphasize the use of the suppression system and minimize the influence of task-learning during the experiments. In these figures, the red line corresponds to the task to be followed by the pilot, while the blue line is the real trajectory commanded.



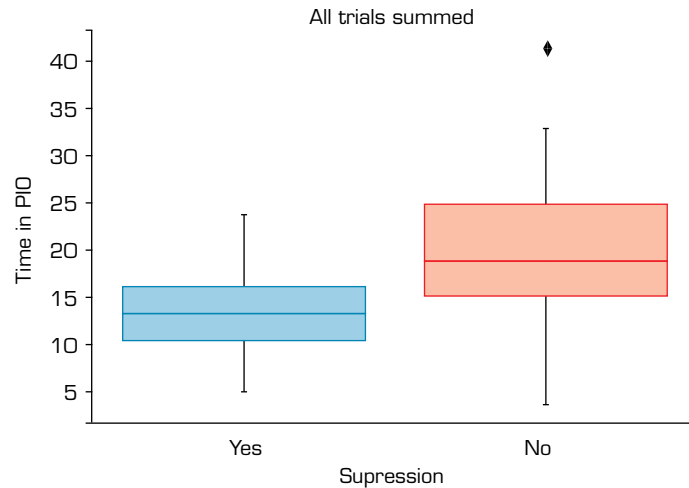
Source: Elaborated by the authors.

Figure 6. Temporal data from one of the volunteers without (a) and with (b) the suppression system.

Figure 6 highlights some regions (circled) of the graphics where there is a significant difference in the behavior compared to the amplitude of the oscillation, reinforcing the influence of the system on flying qualities and the pilot's actions. For all the volunteers, the results followed the same tendency.

Another critical evaluation is based on the general behavior of the volunteers, comparing their results with and without the suppression system. The metric used for this evaluation is based on the amount of time that the ROVER algorithm is set to TRUE in each trial, measuring the time that the pilot-aircraft set was in a PIO condition.

A general analysis in Fig. 7 presents a boxplot comparing all trials with and without the suppression system (in each case, 10 pilots, with five trials each).

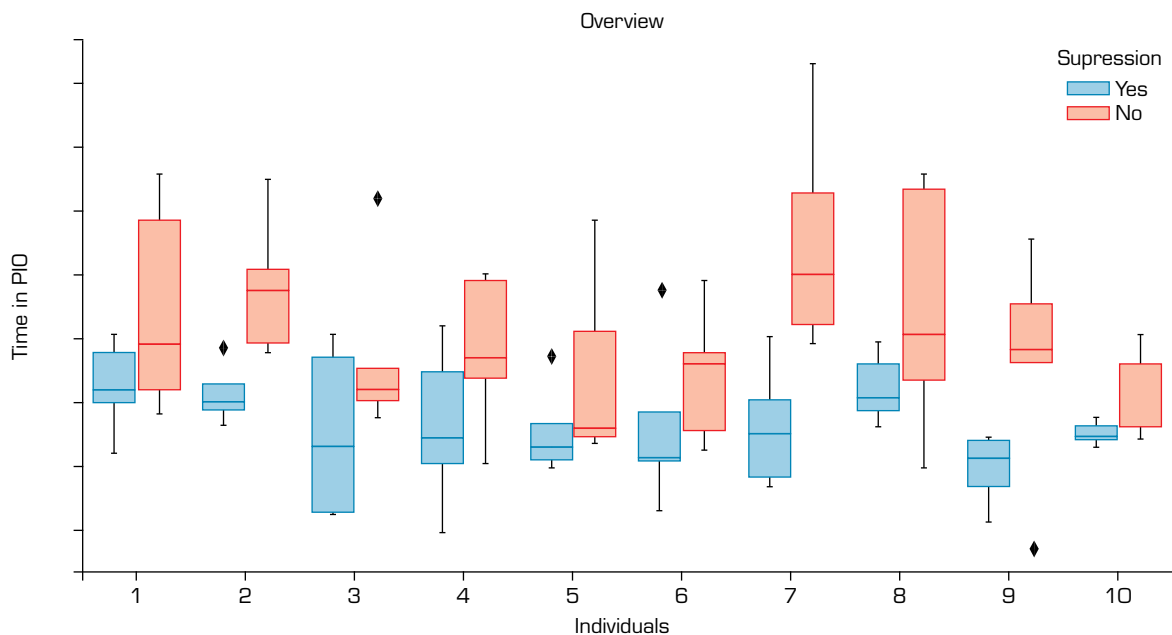


Source: Elaborated by the authors.

Figure 7. Comparison between the trials using and not using the suppression system.

In Fig. 7, it is clear that the use of the suppression system considerably decreases the amount of time in a PIO condition, as well as the variation among the pilots. The blue box, representing the trials with the use of the system, shows considerably lower medians and smaller interquartile ranges.

To demonstrate this tendency for each pilot separately, a set of boxplots was generated to compare each pilot's behavior during the task and the amount of time spent in the PIO condition, as presented in Fig. 8.



Source: Elaborated by the authors.

Figure 8. Boxplot showing the amount of time in PIO condition for each volunteer.

In Fig. 8, when comparing the performance of the system for each volunteer separately (the blue box compared to the orange box for each individual), the same tendency is observed. The blue boxes for each pilot generally present lower medians, and in almost all cases, the interquartile ranges are smaller than those in the orange boxes, which validates a clear tendency of less PIO when the suppression system is used.

In general, it is possible to confirm that using the system tends to decrease the oscillations' amplitude commanded by the pilot when accomplishing a task, as seen in Fig. 6, as well as a smaller amount of time in a condition classified as PIO, seen in the medians observed in Figs. 7 and 8, besides a more regular behavior of the pilots, seen in interquartile ranges in Figs. 7 and 8, without compromising the flying qualities of the aircraft.

CONCLUSION

This work proposed an adaptive system for PIO suppression based on switching of aircraft dynamics, which is feasible for flight controls equipped with FBW systems. Ten volunteers tested the functionality with promising results, as the system could detect the PIO condition in real time and trigger the suppression system. The use of the system consistently reduced the amplitudes during a task accomplishment, and the amount of time on PIO condition is diminished, as well as the variation of behavior among different pilots accomplishing the same task.

For future work, the authors propose (i) using of this system in a moving base flight simulator, (ii) adapting the system to different flight conditions, and (iii) developing the system to possible lateral PIO conditions.

The results were considered consistent and promising, and can positively impact flight safety regarding between pilot-aircraft interaction.

CONFLICT OF INTEREST

Nothing to declare.

AUTHORS' CONTRIBUTION

Conceptualization: Bidinotto JH; **Methodology:** Bidinotto JH; **Software:** Bidinotto JH and Miranda RM; **Validation:** Bidinotto JH and Miranda RM; **Formal analysis:** Miranda RM; **Investigation:** Bidinotto JH and Miranda RM; **Resources:** Bidinotto JH; **Data Curation:** Miranda RM; **Writing - Original Draft:** Miranda RM; **Writing - Review & Editing:** Bidinotto JH and Miranda RM; **Visualization:** Bidinotto JH and Miranda RM; **Supervision:** Bidinotto JH; **Funding acquisition:** Bidinotto JH; **Final approval:** Bidinotto JB.

DATA AVAILABILITY STATEMENT

The data will be available upon request.

FUNDING

Not applicable.



ACKNOWLEDGMENTS

The authors thank the University of São Paulo for the Scientific Initiation scholarship granted under the PUB Program (USP Unified Scholarship Program).

REFERENCES

- [USDoD] U.S. Department of Defense (1995) Flying qualities of piloted airplanes MIL-STD-1797A. Washington D.C.: USDoD.
- Anderson MR (1998) Pilot-induced oscillations involving multiple nonlinearities. *J Guid Control Dyn* 21(5):786-791. <https://doi.org/10.2514/2.4307>
- Ashkenas IL, Jex HR, McRuer DT (1964) Pilot-induced oscillations: their cause and analysis. Technical report. DTIC Document no. STI-TR-239-2. Inglewood: Systems Technology, Inc.
- Bidinotto JH, Almeida SP (2021) A historical review of pilot induced oscillation (PIO) occurrence. Paper presented 26th International Congress of Mechanical Engineering. COBEM/ABCM; virtual congress. <https://doi.org/10.26678/ABCM.COBEM2021.COB2021-0307>
- Bidinotto JH, Moura HC, Macedo JPCA (2022) A survey of human pilot models for study of pilot-induced oscillation (PIO) in longitudinal aircraft motion. *Aeronaut J* 126(1297). <https://doi.org/10.1017/aer.2021.82>
- Chase WD (1967) Piloted simulator display system evaluation: effective resolution and pilot performance in landing approach. Paper presented Third Annual NASA-University Conference on Manual Control (NASA SP-144). NASA; Los Angeles, USA.
- Etkin B, Reid LD (1996) Dynamics of flight: stability and control. Hoboken: John Wiley & Sons.
- Harmin M, Cooper J (2011) Aeroelastic behaviour of a wing including geometric nonlinearities. *Aeronaut J* 115(1174):767-777. <https://doi.org/10.1017/S0001924000006515>
- Johnson DA (2002) Suppression of pilot-induced oscillation (PIO) (master's thesis). Wright-Patterson: Air Force Institute of Technology.
- Lee B (2000) Recent experience in flight testing for pilot induced oscillations (PIO) on transport aircraft. *Aeronaut J* 104(1038):391-395. <https://doi.org/10.1017/S000192400006406X>
- Liu Q (2012) Pilot-induced oscillation detection and mitigation (master's thesis). Cranfield: Cranfield University.
- Mitchell DG, Arencibia AJ, Munoz S (2004) Real-time detection of pilot-induced oscillations. Paper presented AIAA Atmospheric Flight Mechanics Conference and Exhibit. AIAA; Providence, USA. <https://doi.org/10.2514/6.2004-4700>
- Mitchell DG, Hoh RH (1994) The measurement and prediction of pilot-in-the-loop oscillations. AIAA-94-3670-CP. Lomita: Hoh Aeronautics, Inc.
- Moura HC (2018) Supressão adaptativa de PIO em sistemas FBW (master's thesis). São Carlos: Universidade de São Paulo. Available in: <https://www.teses.usp.br/teses/disponiveis/18/18161/tde-27012020-112312/>
- Moura HC, Alegre GSP, Bidinotto JH, Belo EM (2018) PIO susceptibility in fly-by-wire systems. Paper presented 31st Congress of the International Council of the Aeronautical Sciences. ICAS/ABCM; Belo Horizonte, Brazil.

Paladini ALA, Drewiacki D, Bidinotto JH (2024) Aeroelastic effects in PIO occurrences: a dual approach on flight simulator tests. *Aerosp Sci Technol* 151:109337. <https://doi.org/10.1016/j.ast.2024.109337>

Smith JW, Berry DT (1975) *Analysis of longitudinal pilot-induced oscillation tendencies of YF-12 aircraft*. Washington D.C.: NASA.

Sun H, Yu J, Zhang S (2016) The control of asymmetric rolling missiles based on improved trajectory linearization control method. *J Aerosp Technol Manag* 8(3). <https://doi.org/10.5028/jatm.v8i3.617>

Tran AT, Sakamoto N, Kikuchi Y, Mori K (2017) Pilot induced oscillation suppression controller design via nonlinear optimal output regulation method. *Aerosp Sci Technol* 68. <https://doi.org/10.1016/j.ast.2017.05.010>

